Extrapolating HST Lessons to NGST

By Richard G. Lyon, J.M. Hollis, John E. Dorband, and Timothy P. Murphy

TO CORRECT FOR PROBLEMS WITH THE ORIGINAL HST OPTICAL SYSTEM, NASA SCIENTISTS USED PHASE RETRIEVAL TECHNIQUES. HOW THAT WAS DONE AND HOW RESULTS FROM THIS RESEARCH LED TO NASA'S DECISION TO USE IT WITH NGST ARE DISCUSSED.

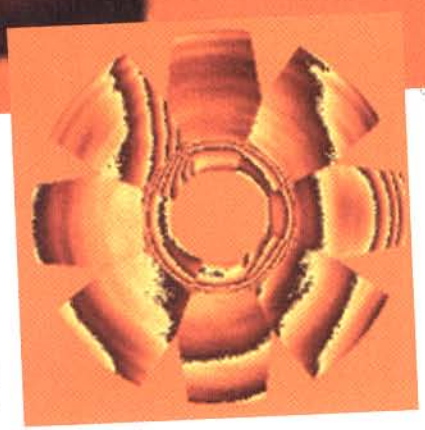

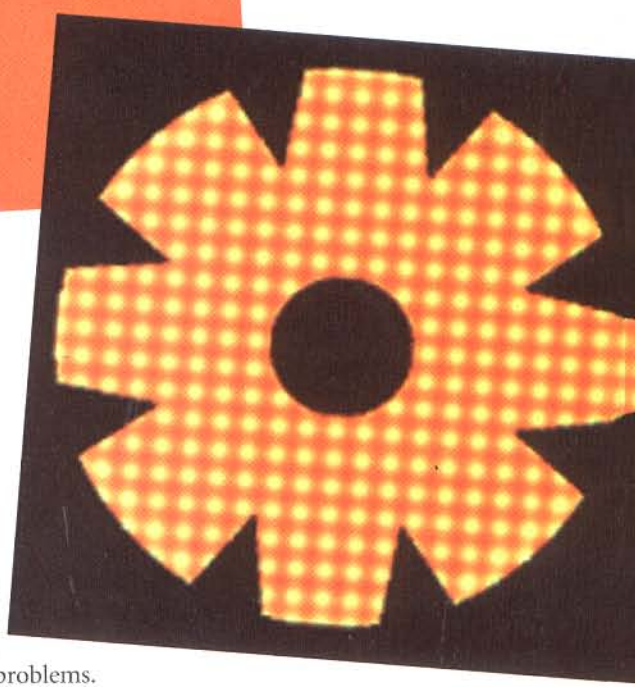

As soon as the initial images were transmitted back to Earth from the Hubble Space Telescope (HST), it was apparent that there were problems with HST's optical system. In response, NASA set up the Optical Systems Characterization and Analysis Research (OSCAR) project at NASA/Goddard Space Flight Center's Earth and Space Data Computing Division. In this division, research is conducted on applying massively parallel computers and computational techniques to solve complex optical, imaging, and data analysis problems.

In a perfect optical system and under ideal conditions (*e.g.*, no Earth atmosphere) a single star illuminates the telescope pupil with a uniform plane wave. This produces an image called the point spread function

1047-6938/98/7/0035/05-$0015.00

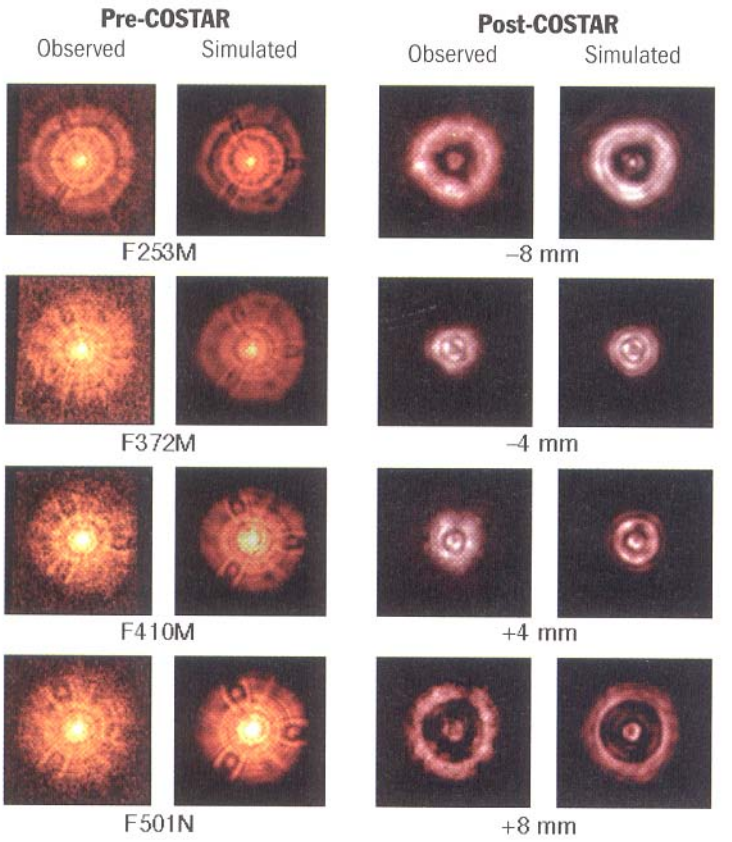

Figure 1. HST phase retrieval results. The first column shows a set of four pre-Corrective Optics Space Telescope Axial Replacement (COSTAR) observed faint object camera (FOC) stellar images (point spread functions or PSFs). Note the wide dynamic range, and hence, non-stationary signal-to-noise ratio. The second column is a set of Lyon electro-optical (LEO) modeled PSFs using phase retrieval to find the wavefront error. The numbers correspond to the filter number (*e.g.*, F253M means the 253-nm filter; M means medium band, and N means narrowband). Note the level of detail in the simulated PSFs that is partially "washed" out in the observed PSFs. The third column shows a set of four post-COSTAR through focus observed PSFs, and the last column displays a set of LEO modeled post-COSTAR PSFs. This set matches the observed set in nearly every detail. The numbers correspond to the position of the deployable optical bench, which verifies that a consistent unified wavelength independent model of both the pre- and post-COSTAR HST optical system exists.[10]

(PSF) at the focal plane. Assume the telescope is in space above the atmosphere. If the characteristics of the PSF indicate that the pupil is non-uniformly illuminated, then this non-uniformity must be caused by aberrations (imperfections) of the optical system. These aberrations, as defined in relation to the telescope pupil plane, are referred to as wavefront errors.

The OSCAR group recognized early on that massively parallel computers could quickly and efficiently calculate accurate mathematical models of the HST optical system to deduce its wavefront error using phase retrieval techniques. This, in turn, led to calculating the noiseless PSFs necessary for performing optimal image deconvolution. The success of these methods provided the rationale for adopting phase retrieval as the baseline wavefront sensing method for studying the alignment and fine figure control of the Next Generation Space Telescope (NGST).[1–3]

After explaining phase retrieval, this article will discuss the HST developments that led to exploring phase retrieval, what studies have been completed for deploying it with NGST, and where OSCAR is currently in terms of the NGST optical system design.

Optical systems modeling and phase retrieval

Phase retrieval is essentially a method of finding the wavefront error in an optical system from an ensemble of observed focal plane images. Wavefront error can result from a variety of causes, including aberrations due to design residuals, fabrication errors, polish marks, alignment errors, and/or thermal and structural drift. In phase retrieval techniques, the inputs are observed images of a narrowband unresolved source such as the HST example in the left column of Figure 1. The output is the wavefront error in the optical systems exit pupil. An output example of two wavefront maps is shown in the lower right of Figure 2 (page 37). The left map is a phase retrieval result using only a single input PSF, while the right map is from simultaneously phase retrieving nine PSFs with a diversity of both focus and wavelength. It is the mid- to high-spatial frequency wavefront that gives the fine detail in the PSFs of Figure 1.

The phase retrieval method of wavefront sensing is akin to interferometry, but with the advantage that, in principle, no additional hardware is required. A science camera is used to generate the input images and, therefore, inherently has the aberrations associated with the entire optical train. Interferometry, on the other hand, requires its own complex, flight qualified optics that must be calibrated; generally, a science camera cannot be used. Hence, this method does not "see" the entire optical train, requiring higher optical tolerances on the instrument.

Compared to interferometry, phase retrieval trades a hardware for a software solution. However, phase retrieval algorithms are nonlinear and, therefore, computer runs are non-deterministic in time. Moreover, phase retrieval requires on the order of 10^{12} floating-point operations and a validated high fidelity computer model of the entire optical system. Further, the algorithm, under some conditions, may not converge to a single solution. The phase retrieval output wavefront is the result of an arctangent function and, thus, is "wrapped" to values between $-\pi$ and π. Research is being done to find robust techniques for unwrapping the wavefront to its true range of values. NASA is in the process of investigating methods of guaranteeing convergence while minimizing processing time. In addition, the NGST work will investigate a number of different algorithms, and apply them in a Monte-Carlo fashion to determine the best approach.

The beginnings of OSCAR

Prior to the HST launch in 1990, phase retrieval was proposed[4] as a backup method in the event that one or more of the three on-board wavefront sensors of the HST failed. It was shown that modest amounts of focus, coma, and astigmatism could be determined by imaging unresolved stars, through narrowband filters, onto the

focal planes of the faint object and wide-field planetary cameras. Considering only misalignment dependent aberrations and exploiting the different field locations of the cameras and different combinations of one or more of the on-board interferometers, the field dependence of the aberrations could be determined to align the HST's secondary mirror.

Phase retrieval was resurrected following the discovery of the HST primary mirror conic constant error and its consequent spherical aberration of the telescope. Outside the dynamic range of the on-board wavefront interferometers, the amount of spherical aberration was determined by a number of different research groups[5–8] using various phase retrieval methods. Further refinement of phase retrieval also led to consistent signatures for misalignment-dependent aberrations and to HST optical prescription predictions for the Corrective Optics Space Telescope Axial Replacement (COSTAR) mission.[9] Even finer refinement determined the combined phase errors due to the residual polish marks on the HST primary and secondary mirrors.[10, 11]

It is the characterization of these polish marks that eventually led to a unified consistent model for the telescope, with enough accuracy to calculate pre-COSTAR PSFs, and enough fidelity for reliable image deconvolution[12, 13] to subsequently predict post-COSTAR PSFs.[8] Figures 1 and 2 are graphic synopses of these results. One of the technological legacies of the HST is the adoption of phase retrieval methods as the NGST baseline wavefront sensing method. Moreover, phase retrieval may be used to determine the initial on-board alignment of NGST optics, as well as to periodically maintain fine figure control.

Forward modeling

To test the various NGST phase retrieval methods, the Lyon electro-optical (LEO) modeling and analysis package has been developed. LEO, previously used to simulate imagery for the HST faint object and wide-field planetary cameras, is currently being used to simulate imagery for the Deployable Cryogenic Active Telescope Testbed (DCATT)[14] and for NGST. The program incorporates

- Multiple plane diffraction, Fresnel, Fraunhofer, and rigorous angular spectrum
- Segmented apertures and obscurations
- Full- and sub-aperture Zernike polynomials (*i.e.*, for the latter, each segment can have its own set with the center and normalization radius arbitrary)
- Random power law surfaces with high and low and cutoffs, integrated root mean square (r.m.s.) power, and a power spectral density slope (which generates speckle in focal plane)
- White noise, and harmonic- and low-frequency jitter models
- Deformable mirror influence function models, quantization error, and range limits
- Detector modulation transfer function, charge transfer efficiency, pixelization effects, quantization error, and dynamic range effects
- Gaussian and Poisson noise models
- System radiometry, specific star color temperature, spectral filter functions, optics transmission, and quantum efficiency
- Some extended scene modeling capability as "seen" through the optical system
- Generic coronagraphic capability with assortment of masks and Lyot stops.

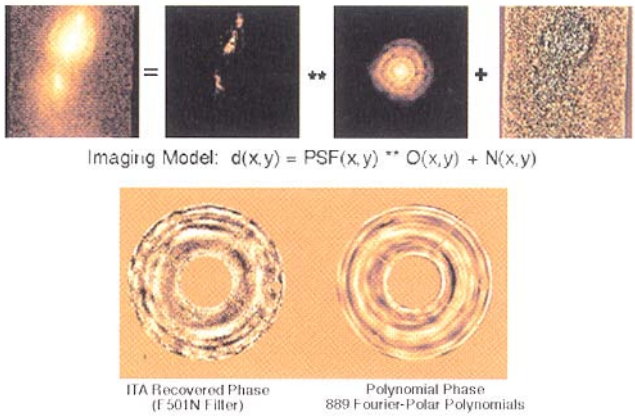

Figure 2. HST maximum entropy image deconvolution and residual wavefront. In the top row, a maximum entropy restoration of an HST/faint object camera image with LEO calculated PSFs. The first image is the raw faint object camera image at 253 nm; the second, the MEM/MLE restoration.[13] The third image is the LEO modeled PSF, and the last is the residual noise frame generated by convolving the restored image with the simulated PSF, subtracting it from the observed data, and then weighting it by the noise standard deviation on a pixel-by-pixel basis. Ideally, the residual noise frame should be entirely de-correlated, however, some residual structure is evident, showing that the deconvolution process is less than perfect.

LEO output can take the form of monochromatic or polychromatic point spread functions (see Fig. 1); point response functions, with detector effects folded in; complex pupils functions, including amplitude and phase (wavefront error); optical transfer and modulation transfer functions, both single wavelength and monochromatic; surface-to-surface raytrace on high density grids (*e.g.*, 1024 × 1024, possibly higher); and output "scenes" as seen through the entire imaging system.

LEO is entirely written in MPL, a massively parallel superset of the C language. LEO runs extremely fast, generally taking less than one second to execute a 15 optical element system. It performs 40 surface-to-surface diffraction calculations/second. It currently runs on Goddard Space Flight Center's MasPar MP2 computer, a massively parallel computer engine consisting of 16,384 separate processors with an associated communications grid. LEO can use adjustable array sizes, with the baseline being 512 × 512. Thus, it can raytrace grids of 512 × 512 rays and perform 512 × 512 fast Fourier transforms (FFTs).

Glossary

Baseline wavefront sensing: In the context used here, "baseline" refers to the main method that will be studied and against which all other methods will be compared.

Deployable Cryogenic Active Telescope Testbed (DCATT): A NASA experimental telescope with a segmented primary mirror that will be used to test some of the design ideas of NGST.

Faint Object Camera (FOC): An HST scientific instrument.

Massively parallel computer: A computer in which over 1,000 processors can operate simultaneously.

Inverse modeling

Currently a number of phase retrieval algorithms are coded and operational; NASA is in the process of quantitatively studying the accuracy and precision of each algorithm. Some of problems that need to be addressed are the effects of jitter; finite sampling, pixel size, and spectral passband; convergence and stagnation issues; phase unwrapping; and effects due to segmented optics and active optics. NASA is also studying whether any significant advantage can be gained by performing phase retrieval in an autonomous control loop, on-board a spacecraft, with minimal or no ground communications.

The NGST wavefront sensing and optical control system

The NGST will most likely be an 8-m aperture telescope, operating at least over the 1.0–5.0 μm wavelength band, and diffraction limited (λ/14) at 2 μm (see Fig. 3). The size and weight constraints for NGST dictate that the primary mirror be lightweight and multi-segmented. Some of the main technological challenges will be to initially phase the segments, maintain the segment alignment, and, in general, maintain the alignment and figure control of the whole optical train. This can be quite a daunting task in orbit. Thus, a phase retrieval based optical control system will be studied, simulated, optimized, and tested on a ground testbed.

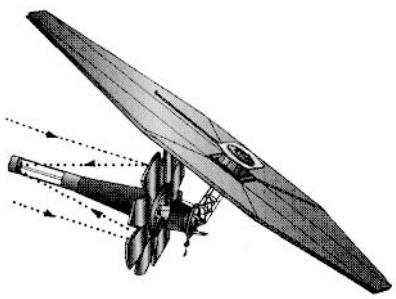

Figure 3. In this Goddard Space Flight Center/Jet Propulsion Laboratory design for NGST, light enters from the upper left, reflects off the segmented primary mirror to the monolithic secondary mirror, and then into the instrument aperture. This telescope design has a large sun-shield (top); the electronics packages are in the center of the sun shield. There is no active thermal control system on NGST as there is on HST and thus the primary mirror temperatures could range from 30–70 K with relatively strong thermal gradients.

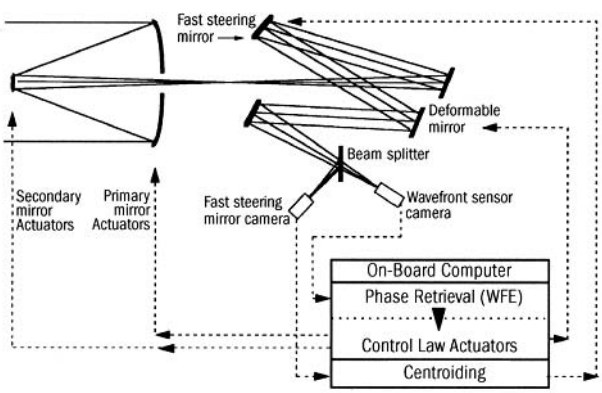

Figure 4. NGST and DCATT conceptual on-board optical control loop. Each of the primary mirrors will move in piston and tip/tilt mode, the secondary mirror will move as a rigid body with six degrees of freedom. The primary mirror is re-imaged onto the deformable mirror and also onto a wavefront sensor. The prime focus of the telescope is relayed through the optical system to both a fast steering mirror and wavefront sensor camera. The fast steering mirror camera is essentially a quad cell detector that centroids the PSF and feed forwards commands to the fast steering mirror. Thus, the fast steering mirror tips and tilts to maintain the position of the PSF on the output camera detector array. This compensates for system jitter. The wavefront sensor camera, essentially the science instrument camera, measures a sequence of images at various foci. The resulting set of images are phase retrieved and actuator commands are generated and fed to the deformable, primary, and secondary mirrors.

This study will first be done in a pure computing environment; then, a subset of the methods studied will be tested in a hardware configuration on the DCATT,[14] and eventually on a technology demonstration flight mission known as Nexus.[15] The Nexus mission will be a segmented aperture telescope adopting the optimal phase retrieval based optical control system tested on DCATT. This will be a validation flight for the final design of the NGST wavefront sensing and optical control system.

Figure 4 is a schematic of one possible NGST optical control loop. The telescope entrance pupil is imaged onto the deformable mirror via an off-axis parabola, and the telescope's cassegrain focus is relayed to the wavefront sensor and fast steering mirror cameras. The fast steering mirror camera is a quad-cell motion detector that provides positioning data for the fast steering mirror control system. The fast steering mirror is driven to keep the image stationary on the wavefront sensor camera and other science instruments in the presence of jitter in the telescope structure. The wavefront sensor camera collects an image (or set of images) and passes them through the phase retrieval software system to recover the wavefront errors. The wavefront errors are then used to determine optimal actuator steps to minimize the wavefront error and commands are sent to the primary and secondary mirrors and to the deformable mirror actuators.

NASA has currently modeled the NGST from an optical systems point-of-view, including the telescope baseline design, a generic science camera, wavefront sensing, and the optical control loop. This baseline model will be used to perform a number of parametric trade studies, as well as a number of different phase retrieval based wavefront sensing options and different actuator based control loops. We are able to model the operational scenario and to investigate a number of different paths to minimize the r.m.s. wavefront errors. Figure 5 shows the phase retrieval based control loop. Two observed PSFs, one on each side of focus, are input to a phase retrieval method. The resultant wavefront is recovered and input to a phase unwrapping algorithm. This resultant wavefront is fit to the deformable mirror actuator influence functions, and the deformable mirror surface is moved to compensate for the error by bringing the wavefront error down to 0.05 wave. Note the waffling in the deformable mirror corrected wavefront, due to the underlying actuators.

A number of the studies have been conducted, or are currently in progress, and will be briefly mentioned here. Different sequences of actuation on the primary

and secondary mirrors and deformable mirror combination are considered. For example, one trade off study will address whether the primary mirror segments should move only in piston and tip/tilt while the higher order aberrations are corrected by the deformable mirror, or, alternatively, whether the primary mirror should also correct higher order modes with and without a deformable mirror. There are other issues as well. For example, would it be better to thermally control the primary mirror and possibly the secondary mirror; how can we continuously monitor image quality; what control scenario minimizes the "waffling" introduced due to the deformable mirror; how can we fold in trend data to the control loop; and what can be gained, from a scientific point-of-view, by performing the wavefront sensor and optical control system autonomously onboard the spacecraft without any operator/analyst in the loop? This latter aspect would reduce the telemetry bandwidth for the periodic alignment process and possibly allow alignment to more often maintain higher image quality throughout the mission's life. Also, due to potentially long thermal settling times, it may be better to actively control the optics during and following a change of the telescope pointing as opposed to letting the optics come to equilibrium then correcting them. Also, how much better image quality can we obtain by using very high density deformable mirrors (~10,000 to 20,000 actuators) and/or a segmented aperture deformable mirror? NASA has also been modeling coronagraphic options and different methods of wavefront sensing through the coronagraph. There are a myriad of challenges, but we believe phase retrieval is up to the task.

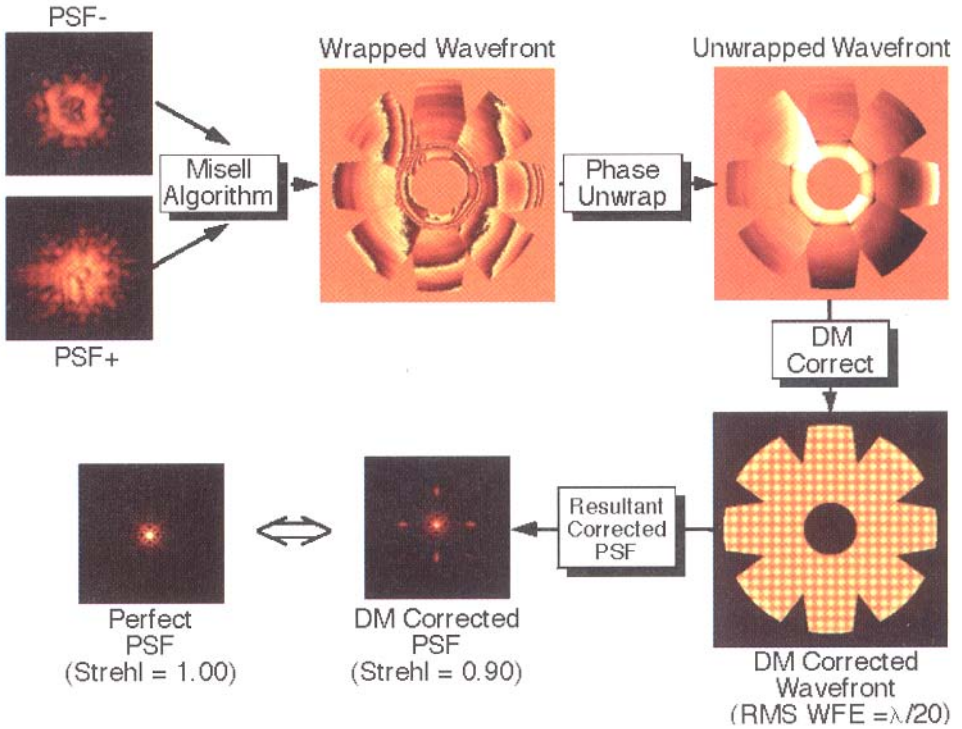

Figure 5. NGST phase retrieval based optical control loop simulation. In the upper left, two input PSFs, one on each side of focus, are input to a Misell phase retrieval algorithm. In the upper middle, the phase retrieval output is the entire optical trains wavefront error. This is returned modulo 2π, unless the wavefront error is less than 1 wave. In the upper right is the unwrapped wavefront error. Note that each segment can have its own errors. This simulation also contains residual polish marks and surface micro-roughness. In the lower right, the unwrapped wavefront is fit to the actuator influence functions and the deformable mirror moved to correct the wavefront. Shown is the residual "quilt" pattern. The deformable mirror corrected wavefront is $\lambda/20$ r.m.s. wavefront error. In the lower middle is the resultant deformable mirror corrected PSF. Note that this is logarithmically stretched to bring up some of the residual background structure. The lower left shows the perfect PSF, *i.e.*, with no wavefront error in the entire system for comparison. This also has the same logarithmic stretch as the deformable mirror corrected PSF.

References

1. B.D. Seery, "Next Generation Space Telescope (NGST)," Proc. SPIE **3356,** (SPIE Press, Bellingham, Wash., March 1998) Kona, Hawaii.
2. J.C. Mather and P. Stockman, "NGST: Technology for Looking Back in Time," Proc. American Astronomical Society, Bulletin of the American Astronomical Society **191,** (American Institute of Physics, Woodbury, N.Y., 1997) session 54, paper 2.
3. D. Redding *et al.*, "Wavefront Sensing and Control for a Next Generation Space Telescope," Proc. SPIE **3356,** (SPIE Press, Bellingham, Wash., March 1998) Kona, Hawaii.
4. L.G. Grey and R.G. Lyon, "Correction of Misalignment Dependent Aberrations of the Hubble Space Telescope via Phase Retrieval," Proc. SPIE **1168,** (SPIE Press, Bellingham, Wash., Aug. 1989) San Diego, Calif.
5. R.G. Lyon *et al.*, "Hubble Space Telescope Phase Retrieval: A Parameter Estimation," Proc. SPIE **1567,** (SPIE Press, Bellingham, Wash., July 1991) San Diego, Calif.
6. D. Redding *et al.*, "Hubble Space Telescope prescription retrieval," Appl. Opt. **32** (10), 1993.
7. C.J. Burrows, "Hubble Space Telescope Optics Status," Proc. SPIE **1567,** (SPIE Press, Bellingham, Wash., July 1991) San Diego, Calif.
8. J.R. Fienup, "Phase Retrieval for the Hubble Space Telescope Using Iterative Propagation Algorithms," Proc. SPIE **1567,** (SPIE Press, Bellingham, Wash., July 1991) San Diego, Calif.
9. H.J. Wood, "Hubble Space Telescope: Mission update," Opt. & Phot. News **5** (8), 8–13 (1994).
10. R.G. Lyon *et al.*, "Hubble Space Telescope faint object camera calculated point spread functions," Appl. Opt. **36** (8), 1752–1765 (1997).
11. J.E. Krist and C.J. Burrows, "Phase retrieval analysis of pre- and post-repair Hubble Space Telescope images," Appl. Opt. **34** (22), 4951–4964 (1995).
12. J.M. Hollis *et al.*, "Spatial resolution of the R-aquarii binary system," APJ L **488,** 85–88 (1997).
13. J.M. Hollis *et al.*, "Motion of the ultraviolet R-aquarii jet," APJ, **475,** 231–236 (1997).
14. C. Lebeouf *et al.*, "Deployed Cryogenic Active Telescope Testbed for the Next Generation Space Telescope," Proc. SPIE **3356,** (SPIE Press, Bellingham, Wash., March 1998) Kona, Hawaii.
15. L. Pacini *et al.*, "Nexus: The Next Generation Space Telescope Integrated Flight Systems Demonstration," Proc. SPIE **3356,** (SPIE Press, Bellingham, Wash., March 1998) Kona, Hawaii.

Richard G. Lyon is a research scientist and Timothy P. Murphy is a research associate at NASA's Center of Excellence in Space Data and Information Sciences. Both are associated with the electrical engineering department at the Univ. of Maryland, Baltimore County, Greenbelt, Md. J.M. Hollis is an astrophysicist and assistant division chief and John E. Dorband is a computer scientist at the Earth and Space Data Computing Division, NASA/GSFC, Greenbelt, Md.